Applied Catalysis B: Environmental 88 (2009) 430–437

Contents lists available at ScienceDirect

Applied Catalysis B: Environmental

journal homepage: www.elsevier.com/locate/apcatb

Oxidation of CH_4 over Pd supported on TiO_2-doped SiO_2: Effect of Ti(IV) loading and influence of SO_2

A.M. Venezia [a,*], G. Di Carlo [b], G. Pantaleo [a], L.F. Liotta [a], G. Melaet [c], N. Kruse [c]

[a] Istituto dei Materiali Nanostrutturati (ISMN-CNR) via Ugo La Malfa 153, Palermo I-90146, Italy
[b] Dipartimento di Chimica Inorganica ed Analitica "Stanislao Cannizzaro", Università di Palermo, Viale delle Scienze, Palermo I-90128, Italy
[c] Université Libre de Bruxelles (ULB) Chemical Physics of Materials, Campus de la Plaine, C.P. 243, Bld du Triomphe, B-1050 Bruxelles, Belgium

ARTICLE INFO

Article history:
Received 14 July 2008
Received in revised form 16 October 2008
Accepted 25 October 2008
Available online 8 November 2008

Keywords:
Methane combustion
TiO_2/SiO_2 supports
PdO catalyst
SO_2 effect

ABSTRACT

Titania-modified silicas with different weight% of TiO_2 were prepared by sol–gel method and used as supports for Pd (1 wt%) catalysts. The obtained materials were tested in the oxidation of methane under lean conditions in absence and in presence of SO_2. Test reactions were consecutively performed in order to evaluate the thermal stability and poisoning reversibility. Increasing amounts of TiO_2 improved the catalytic activity, with an optimum of the performance for 10 wt% TiO_2 loading. Moreover, the titania-containing catalysts exhibited a superior tolerance towards SO_2 by either adding it to the reactants or feeding it as a pure pretreatment atmosphere at 350 °C. Catalysts were characterized by XPS, XRD, FT-IR and BET measurements. According to the structural and surface analyses, the mixed oxides contained Si–O–Ti linkages which were interpreted as being responsible for the enhanced intrinsic activity of supported PdO with respect to PdO on either pure SiO_2 or pure TiO_2. Moreover, the preferential interaction of the sulfur molecule with TiO_2 and the easy SO_x desorption from high surface area silica were the determining factors for the superior SO_2 tolerance of the TiO_2-doped catalysts.

1. Introduction

Methane or natural gas fuelled engines (NGVs) are presently considered a valid alternative to those fuelled by diesel and gasoline. Several environmental advantages of NGVs are usually cited. First, because of a lower combustion temperature of lean-operated NGV's the emission of NO_x is lower. Second, since the H:C ratio is high in CH_4, the emission of CO_2 is lower than in conventional fuelled vehicles and, third, smaller amounts of particulates in comparison with diesel vehicles are produced [1,2]. However, a major drawback associated with its use is the emission of unburned CH_4, an effective greenhouse gas which contributes to global atmosphere warming even more than CO_2 because of its longer lifetime [2]. Therefore, to comply with modern legislation, highly efficient catalysts for the complete abatement of the unburned methane are needed.

Pd-based catalysts are among the most active ones for methane oxidation at low temperatures [3–4]. As pointed out in several studies, their catalytic activity depends strongly on the nature of the support [3–5], on the palladium precursors [6] and on the size of the PdO particles considered as the active phase [3]. Generally, a detrimental particle sintering occurs in the presence of water and a serious catalyst poisoning is observed in the presence of sulfur compounds [1,5,7]. Interacting supports like alumina and titania, differently from the inert silica, limit the extent of noble metal sintering during reaction therefore preserving the activity for a longer time [8]. With respect to sulfur poisoning, the suitability of sulfating or non-sulfating supports is still a matter of debate [7–9]. According to literature, when a sulfating support like Al_2O_3 is used, palladium deactivates slowly due to the preferential interaction of SO_x with the support. This is at variance with a non-sulfating support like SiO_2 in which case palladium deactivates much faster [8,10]. However, the use of a support like silica allows an easier regeneration of the sulfur-poisoned catalyst through the thermal decomposition of the palladium sulfate [8,11]. Recently, our group reported a silica-supported Pd catalyst providing high methane conversion and only slight deactivation by SO_2 [10]. The silica used had the HMS mesoporous structure characterized by a high surface area and a well controlled pore size. In the presence of SO_2 the HMS-supported catalyst deactivated to a lesser extent as compared to the case of a "PdO" supported on an amorphous and lower surface area silica. A complete recovering with a remarkable enhancement of the catalytic activity with respect to the fresh sample was observed in a subsequent run without SO_2. This quite

* Corresponding author. Tel.: +39 0916809372; fax: +39 0916809399.
E-mail address: anna@pa.ismn.cnr.it (A.M. Venezia).

0926-3373/$ – see front matter © 2008 Elsevier B.V. All rights reserved.
doi:10.1016/j.apcatb.2008.10.023

surprising behavior was attributed to the particular morphology of the support which acted essentially as a sponge for the SO_2 species. Only a small portion of the SO_2 was adsorbed on "PdO" thus partly reducing and deactivating it. However, in a following run, after removal of the SO_2 from the feed, the reducing effect of SO_2 on PdO was, by and large, positive thus leading to a structural rearrangement of the active phase.

On these grounds, in the present study, as a continuation of our previous work [10] we aimed to combine the use of a sulfating and of a non-sulfating support in the attempt to obtain a Pd-based catalyst which was more active and completely tolerant towards SO_2 poisoning during methane oxidation. Mixed TiO_2 and SiO_2 oxides in different weight ratios were prepared by a sol–gel procedure and used as supports for PdO. The catalytic performance was investigated and a structural analysis by XRD, XPS, FT-IR and N_2 physisorption (BET) performed.

2. Experimental

2.1. Support and catalyst preparation

The supports were synthesized by the sol–gel method so as to provide homogenous and high surface area samples [12]. Accordingly, SiO_2 and TiO_2 were prepared by hydrolysis using tetraethoxysilanole TEOS and, respectively, titanium isopropoxide, as precursors. Hydrolysis was performed at 45 °C by adding an aqueous solution of acetic acid at pH 5. The product was kept at this temperature for 2 h and then at 80 °C for 1 h. In order to remove the solvent, the gel was dried at 110 °C for 6 h and then calcined at 450 °C for 4 h. Mixed supports with 5, 10, 15 and 20 wt% of TiO_2 were prepared by a modified sol–gel method, starting from the appropriate amount of titanium isopropoxide and TEOS. A mixture of TEOS and titanium isopropoxide was stirred and refluxed at 80 °C to avoid the instant hydrolysis of the titania precursor. Then the aqueous solution of acetic acid was added at 80 °C in order to simultaneously hydrolyse both precursors. The gel was kept at this temperature for 1 h and then dried at 110 °C for 6 h. It was finally calcined at 450 °C for 4 h.

Palladium was deposited by wet impregnation using an aqueous solution of palladium nitrate in amounts ensuring the production of supported catalysts with 1 wt% Pd. The samples were calcined at 400 °C for 4 h. The chemical composition of the samples was checked by X-ray fluorescence analyses. The samples were labelled Pd/SiO_2, Pd/TiO_2 and Pd/TixSi where x stands for the TiO_2 wt%.

2.2. Catalyst characterization

X-ray diffraction patterns were measured with a Philips vertical goniometer using Ni-filtered Cu Kα radiation. A proportional counter and 0.05° step sizes in 2θ were used. The assignment of the various crystalline phases was based on the JPDS powder diffraction file cards [13]. The line broadening of the main reflection peaks was used to determine particle sizes via the Scherrer equation, with a lower detection limit of 3 nm [14].

The microstructural properties of the materials were obtained from N_2 adsorption–desorption isotherms at −196 °C using a Sorptomatic 1900 (Carlo Erba) instrument. Before the measurements, samples were heated in vacuum at 250 °C for 2 h. Specific surface areas and pore size distributions of the materials were obtained using the BET and the BJH calculation methods [15].

The X-ray photoelectron spectroscopy analyses were performed with a VG Microtech ESCA 3000 Multilab, using the unmonochromatised Al Kα source (1486.6 eV) run at 14 kV and 15 mA. For the individual peak energy regions, a pass energy of 20 eV was used. Samples were mounted with a double-sided adhesive tape. Binding energies were referenced to the C 1s binding energy of adventitious carbon set at 285.1 eV. The software provided by VG was used for peak analyses and for the calculation of the atomic concentrations. The precision of binding energies and atomic percentages were ±0.15 eV and ±10%, respectively.

FT-IR spectra of the samples were recorded in absorbance by means of an FT-IR 5300 Jasco spectrophotometer using the KBr wafer technique. The resolution was 4 cm^{-1}.

The point of zero charge (PZC) of the various supports was determined by mass titration [16]. According to this method, the variation of the pH of a water solution containing increasing amounts of solid was monitored until the steady state pH value (PZC) was reached.

2.3. Catalytic activity

Methane oxidation was performed using an U-shaped quartz reactor with an inner diameter of 12 mm, electrically heated in a furnace. The catalyst powder (sieved fraction between 180 and 250 μm) was placed on a porous disk diluting it 1:2 with inert SiC in order to avoid thermal gradients. The reaction temperature was measured by a K-type thermocouple in contact with the catalytic bed of 12 mm height. Prior to catalytic testing, the samples were treated "in situ" under flowing O_2 (5 vol.% in He, 50 ml/min) at 350 °C for 1/2 h and in He during cooling at 200 °C. The standard reagent gas mixture consisting of 0.3 vol.% CH_4 + 2.4 vol.% O_2 in He was led through the catalyst (50 mg) at a flow rate of 50 ml/min (STP), equivalent to a weight hourly space velocity (WHSV) of 60,000 ml g^{-1} h^{-1}. Activities were measured by increasing the temperature from 200 to 600 °C (by steps of 50 °C, holding time 45 min). This particular reaction temperature range was selected on the basis of the operating temperature, typically 320–420 °C, as reported for lean-burn NGVs catalytic converters [1]. The inlet and outlet gas compositions were analyzed by on line mass quadrupole mass spectrometer (Thermostar™, Balzers), in order to follow the evolution with time and temperature of m/e values representative for CH_4, CO, CO_2, H_2, H_2O, O_2. Moreover, the concentration of CO and CO_2 species was checked by an IR analyser (ABB Uras 14), calibrated in the ranges 0–3000 ppm for CO and, respectively, 0–10,000 ppm for CO_2. The reaction products of methane oxidation were CO_2 and H_2O. No CO was detected over the range of temperatures considered here. The carbon balance was close to ±5% in all the catalytic tests. Experiments of methane oxidation in the presence of SO_2 were performed by co-feeding 10 vol. ppm of SO_2. Overnight treatments of the samples, with flowing 10 vol. ppm of SO_2/He and/or 5 vol.% H_2/Ar at 350 °C at a flow rate of 50 ml/min, were also carried out, prior to catalytic tests. Between consecutive runs the samples were cooled down in an inert He atmosphere.

3. Results and discussion

3.1. Catalytic activity with SO_2-free and SO_2-containing reactant mixture

The catalytic activities of the different catalysts are compiled in Table 1 using T_{50} values (which correspond to temperatures of 50% CH_4 conversion) of different runs performed sequentially or not, under varying conditions. The temperature dependence of methane conversions, relative to the first run without SO_2, over the pure oxides and over the Pd mixed oxide-supported catalysts are shown in Fig. 1. Obviously, the mixed oxide-supported samples are more active than Pd/TiO_2 which, in turn, is more active than Pd/SiO_2. The beneficial effect of TiO_2 addition to silica seems to be quite general, with a maximum of the activity occurring at 10 wt% TiO_2.

Table 1
Temperature of 50% methane conversion, T_{50} (°C) over palladium-based catalysts in different conditions.

Conditions	Pd/SiO_2 T_{50} (°C)	Pd/Ti5Si T_{50} (°C)	Pd/Ti10Si T_{50} (°C)	Pd/Ti15Si[a] $0T_{50}$ (°C)	Pd/Ti20Si T_{50} (°C)	Pd/TiO_2 T_{50} (°C)
(Ia) first run: SO_2-free	355	332	312	321	326	337
(Ib) first run: with SO_2	395	379	365	n.a.	381	346
(II) second run: SO_2-free	395	339	330	n.a.	334	388
(III) third run: SO_2-free, after SO_2 pretreatment	411	363	357	n.a.	365	447
(IV) fourth run: SO_2-free	370	298	287	n.a.	291	432

[a] For this sample only the first run was carried out.

In order to study the tolerance against sulfur poisoning, methane was oxidized over fresh samples while co-feeding 10 vol. ppm SO_2. Subsequently a second run with SO_2-free reactants was carried out in order to investigate how the catalyst regenerated from SO_2 exposure. In Fig. 2 the respective temperature-dependent conversion of three selected samples are shown including Pd on pure oxides, SiO_2 and TiO_2, and PdTi5Si. The results of the other PdTi*x*Si catalysts are provided in Table 1. For the sake of clarity, relative curves have been omitted in Fig. 2. Comparing the first run (Ib) of Fig. 2 and the corresponding data for the other samples in Table 1, the order of activity is the following: Pd/TiO_2 > Pd/Ti*x*Si > Pd/SiO_2. As expected, according to the nature of the carrier, the sulfating oxide, TiO_2, imparts good SO_2 tolerance to the "PdO". Indeed, as reported in the literature, SO_2 can adsorb on both, the support and the "PdO" phase including migration via surface diffusion between both [7]. If the sulfating power is stronger for the support than for the noble metal, spillover of sulfate may occur meaning that sulfate eventually formed on "PdO" would spillover onto TiO_2 therefore preserving the "PdO" phase from being heavily poisoned by SO_2. Such mechanism of spillover does not apply to SiO_2 being inert towards sulfation. However, as shown in Fig. 2 and Table 1, in the consecutive run with SO_2-free reactants, while Pd/TiO_2 further deteriorates, Pd/SiO_2 maintains its activity whereas PdTi*x*Si catalysts become even more active. A possible explanation may be as follows. With a pure silica support, sulfates associated with "PdO" are thermally desorbed at the high temperature (600 °C) reached at the end of the previous run [8,10,17], whereas with pure TiO_2, sulfates associated with the support may migrate over to PdO with a consequent decrease of the activity in the subsequent run [11]. The permanent loss of activity still observed with the pure silica-supported catalyst with respect to the fresh sample (Fig. 1), is likely due to some PdO particle sintering [8]. Pd catalysts supported on TiO_2-doped SiO_2 exhibit a superior performance, possibly due to a synergistic effect, with less sintering as in Pd/SiO_2 and less sulfation as in Pd/TiO_2 as they recover almost completely in the following SO_2-free run. It should be mentioned that evolution of water during the reaction could also contribute to the deactivation of the catalysts in synergy with SO_2 [7,18]. The extent of the synergy would depend on the support composition, particularly on the relative amount of sulfatable and not sulfatable oxides. Indeed, as reported in literature [7] the synergistic effect may be explained in two ways: (i) water, adsorbing on the support surface would decrease the amount of SO_2 adsorbed, hence forcing spillover of surface SO_x onto the supported PdO particles; (ii) by the formation of $Pd(OH)_2$ which, as proposed by Burch et al. in [18] is more reactive with sulfur oxides than PdO.

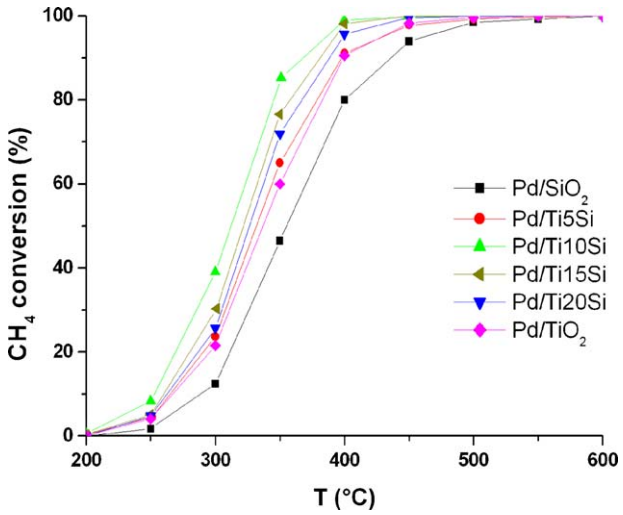

Fig. 1. Methane conversion as a function of temperature over the different catalysts during the first run without SO_2.

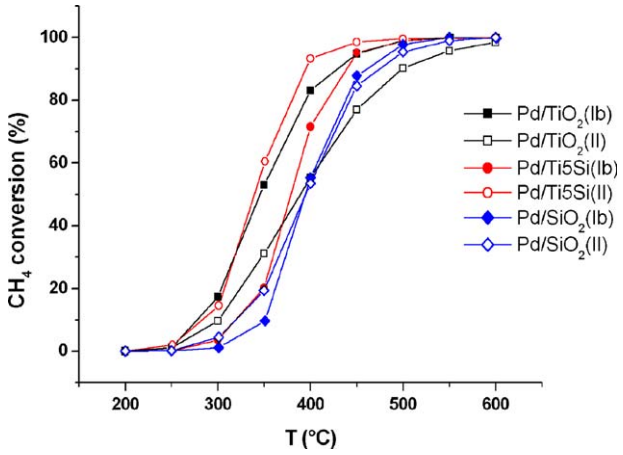

Fig. 2. Methane conversion as a function of temperature over pure oxide-supported catalysts and mixed oxide Pd/Ti5Si during the runs Ib (run with SO_2 in the gas mixture) and the following II (SO_2-free).

3.2. Effect of pretreatment with SO_2 and H_2 on the catalytic activity

To mimic severe poisoning and also rule out any effect associated with water evolution, an isothermal treatment was carried out overnight at 350 °C in flowing 10 vol. ppm of SO_2/He, after the two consecutive runs described above (Ib and II). Thereafter two catalytic tests labeled run III and run IV in Table 1, were performed one after the other. The corresponding conversion curves are compared with those of the previous tests. For the sake of clarity, in Fig. 3 only the results of Pd/Ti10Si are plotted while the data obtained with the other catalysts are compiled in terms of T_{50} in Table 1. Again the poisoning effect depends on the support. Contrary to the situation in which the presence of TiO_2 limited the "PdO" poisoning by SO_2, as compared to pure SiO_2, under the overnight reducing treatment with SO_2/He, the deactivation order is Pd/TiO_2 > Pd/SiO_2 > Pd/TiSi. The differences in the catalytic performance became clearly evident in run IV during which Pd/

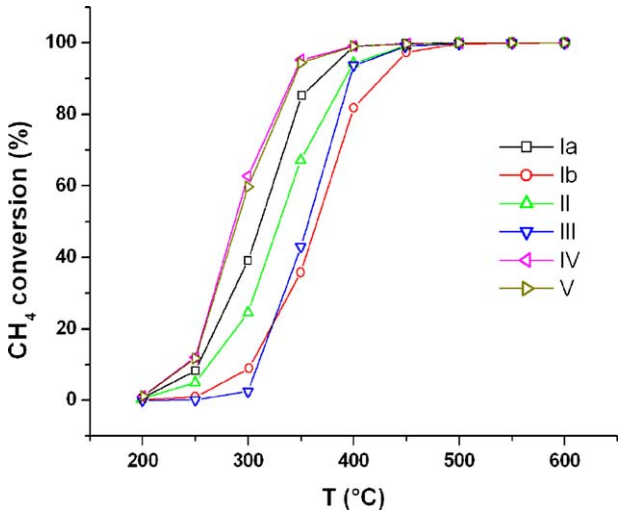

Fig. 3. Methane conversion over Pd/Ti10Si as a function of reaction temperature: curve Ia (first run SO_2-free); curve Ib (first run with SO_2); curve II (second run SO_2-free, after run Ib); curve III (third run SO_2-free, after run II and additional overnight treatment in SO_2); curve IV (fourth run without SO_2 after run III); curve V (fifth run, SO_2-free, after run IV).

SiO_2 recovered largely its activity and all the Pd/Ti*x*Si catalysts became more active, with a maximum of the activity being obtained for Pd/Ti10Si. The remarkable performance of this catalyst was also confirmed in a fifth consecutive run (V) with decreasing temperatures ("downward run"). As shown in Fig. 3, the conversion profile of this run is coincident with the one of increasing temperatures performed before (IV, "upward run") reaching a complete reversibility of the process. The activity enhancement observed in these experiments was already reported in the previous work with Pd/HMS and PdAu/HMS [10]. Then, based on the structural evidence obtained for the gold-promoted catalyst, the activation was attributed to the SO_2-induced reduction and restructuring of PdO particles.

To confirm the role of the SO_2 as a reducing agent, in the present catalysts, additional tests were carried out with the best performing candidate, Pd/Ti10Si, after overnight treatment in H_2. In Fig. 4 comparison is made between runs III, IV and V

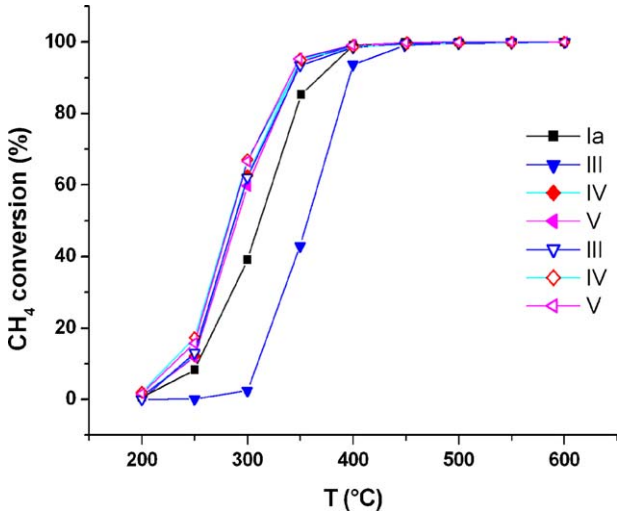

Fig. 4. Methane conversion as a function of temperature over the Pd/Ti10Si: curve Ia (first run SO_2-free); curve III, IV and V refer to the runs after the overnight treatment in SO_2 (full symbols) and in H_2 (open symbols).

performed consecutively after runs Ib and II of Table 1 and after SO_2 or H_2 treatment. For comparison reason the run performed on the fresh sample (Ia) is also reported. It is interesting to note that a H_2 treatment allowed the catalyst to attain the maximum activity already in the third run. This is not too surprising since in this case there was no SO_x to be removed. This test yet simply confirmed that the (re)activation by SO_2 treatment in either presence or absence of oxygen is similar to the hydrogen treatment and therefore associated with the reduction of the PdO phase as suggested earlier [10].

In the previous paper [10] the measurements of the Arrhenius parameters for the Pd over high surface area mesoporous silica before and after sulfur exposure confirmed the idea that the sulfur deactivation was related to the formation of a less active species such as PdO–SO_x corresponding to an increase of the activation energy [17]. The subsequent runs with SO_2-free reagent mixture determined a reactivation of the catalysts in accord with a substantial decrease of the activation energy. On the basis of the Arrhenius parameters obtained from the complete sequence of catalytic tests, such enhancement of the activity was explained in terms of a structural rearrangement caused by the SO_2 exposure. In the present study from the Arrhenius plot of ln (k) versus $1/T$, in the temperature range of 250– 350 °C, corresponding to conversions ranging between 10% and 80%, the (apparent) activation energies E_{act} and the pre-exponential factors A of the Arrhenius equation, $k = A\ exp\ (-E_{act}/RT)$, were calculated. As before, neglecting the effect of small amounts of water formed in the process [8,10] the integral equation of a first order reaction with respect to methane and pseudo-zero order with respect to oxygen was used for the calculation of the reaction rate constants k [8,10]. In Table 2 the Arrhenius parameters obtained from the 1st test on fresh samples (Ia) and from test IV, after several runs and treatments, are compiled for all the catalysts. The two particular tests were selected in order to investigate the final variation of the original active sites upon the consecutive runs performed with and without SO_2. Variations of the activation energies may indeed reflect changes of the active site ensemble. For the 1st run without SO_2, E_{act} values of 84 kJ/mol for Pd/TiO_2 and of 97 kJ/mol for Pd/SiO_2 were obtained. The values for the Pd/TixSi were between the above two values, with the smaller E_{act} values obtained for the most active Pd/Ti5Si and Pd/Ti10Si catalysts. In run IV (as in Table 1), E_{act} decreased for all the samples. As suggested for similar systems [10], at the end of the third run, after several cycles including the overnight SO_2 treatments, a considerable restructuring with modification of the nature of the active sites probably occurs. The large decrease of the pre-exponential factor observed in Pd/TiO_2 reflects also structural changes induced by the reactions, related to different active site concentration and site poisoning. In this case, the presence of SO_2 strongly attached to the support, by spillover would decrease the number of the active PdO sites. In the

Table 2
Activation energy (E_{act}) and pre-exponential factor A relative to the SO_2-free run and to the fourth run of Table 1[a].

Samples	E_{act} (kJ/mol)		ln A	
	First SO_2-free run	Fourth run	First SO_2-free run	Fourth run
Pd/SiO_2	97	74	21	20
Pd/Ti5Si	85	80	19	19
Pd/Ti10/Si	83	74	19	19
Pd/Ti15/Si	90	–	21	–
Pd/Ti20/Si	89	88	20	20
Pd/TiO_2	84	78	19	16

[a] E_{act} and A are calculated from the Arrhenius plot in the temperature range 250–350 °C.

Table 3
BET surface area (S), average pore diameter (D), pore volume (V_p) and zero point charge (ZPC) of the supports. The particle diameters for the supported PdO as obtained from XRD of the fresh catalysts are also given.

Sample	S (m^2/g)	D (nm)	V_p (cm^3/g)	ZPC	d_{PdO} (nm)
SiO_2	688	3.7	0.57	4.5	9
Ti5Si	328	2.1	0.18	4.2	9
Ti10Si	284	2.1	0.20	4.2	8
Ti15Si	243	3.3	0.19	4.3	6
Ti20Si	170	3.7	0.17	4.4	6
TiO_2	38	3.8	0.07	5.9	<3

silica and in the mixed oxide supports such effect is lessened due to the easier removal of SO_2.

3.3. Characterization of fresh and treated catalysts

The variation of the catalytic performance in TiO_2-loaded samples suggests structural changes to be relevant. To provide evidence of such changes, a number of physical and spectroscopic analyses were performed. In Table 3, surface areas and textural properties of the supports are compiled along with points of zero charge and with the PdO particle sizes estimated by XRD measurements carried out on the fresh catalysts. Clearly, the addition of TiO_2 to SiO_2 caused the specific surface area to decrease significantly. This effect although to a less extent was already observed when grafting similar amounts of titania on silica [9,19]. The average pore diameters and pore volume changed accordingly. Slight increase of the surface acidity in the mixed supports as compared to pure SiO_2 are reflected in the ZPC values.

Figs. 5 and 6 show the X-ray diffraction patterns of the fresh samples and of the aged ones (after run IV as in Table 1). All the fresh sample patterns contain a small peak attributed to the (1 0 1) reflection of PdO, with the exception of Pd/TiO_2 where only the main reflections of TiO_2 anatase are observed. From the line width of the PdO peak, according to the Scherrer analysis, the calculated values of the PdO particle size of the fresh samples, given in Table 3, slightly decreases with the increasing of the TiO_2 content. As suggested by the absence of the corresponding peak in Pd/TiO_2, PdO particles in this sample are probably smaller than the instrumental detection limit of 3 nm. As shown in Fig. 6 the PdO peaks in the diffractograms of the aged samples are less intense and asymmetric. The pronounced asymmetry and the decreased intensity of the peaks suggest considerable structural rearrangements to have occurred. In the diffractograms of Pd/TiO_2 and

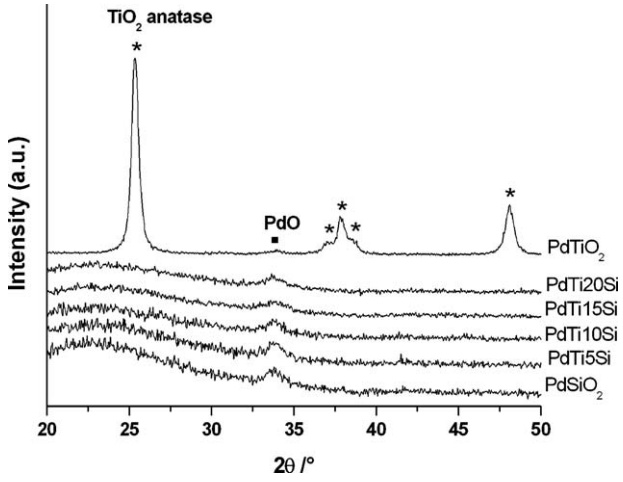

Fig. 5. XRD patterns of the pure and mixed oxide-supported Pd catalysts.

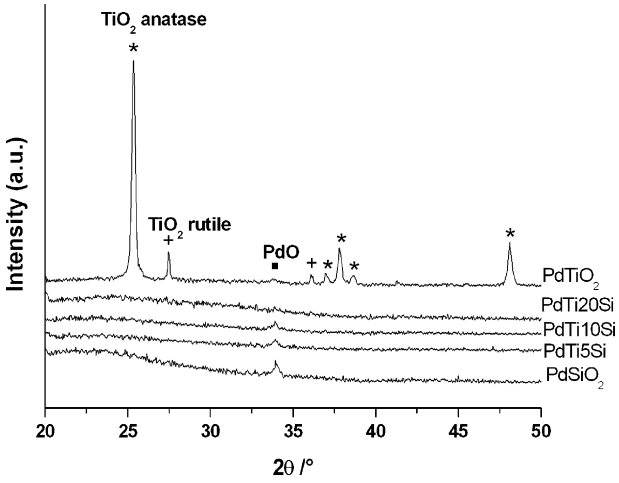

Fig. 6. XRD patterns of the pure and mixed oxide-supported Pd catalysts after run IV.

Table 4
XPS binding energies and XPS-derived atomic ratios of the fresh catalysts.

Sample	Pd $3d_{5/2}$ (eV)	Ti $2p_{3/2}$ (eV)	O 1s (eV)	Ti/Si[a]	Pd/(Ti + Si)[b]
Pd/SiO_2	337.4		533.3		0.008 (0.006)
Pd/Ti5Si	337.3	460.5	533.4 (96%) 531.3 (4%)	0.02 (0.04)	0.03 (0.02)
Pd/Ti10Si	337.5	460.2	533.4 (95%) 531.3 (5%)	0.04 (0.08)	0.03 (0.02)
Pd/Ti15Si	337.3	460.0	533.1 (93%) 531.1 (7%)	0.05 (0.13)	0.009
Pd/Ti20Si	337.4	459.8	533.1 (91%) 531.1 (9%)	0.06 (0.19)	0.005 (0.003)
Pd/TiO_2	336.9	458.9	530.3		0.05 (0.04)

[a] The values in parentheses represent the bulk atomic ratio.
[b] The values in parentheses refer to the aged samples (after the fourth run).

PdTi20Si the PdO peak was hardly visible. Moreover, in the Pd/TiO_2 sample, while a good dispersion of the PdO phase was maintained, the titania underwent a phase transition from anatase to rutile. The high palladium dispersion on the Pd/TiO_2 and Pd/Ti20Si catalysts may be related to the rather strong PdO–TiO_2 interaction [20].

Information on the chemical state and the surface chemical composition of the samples, before and after the catalytic tests, were obtained by XPS analyses. In Table 4 the Pd $3d_{5/2}$, the Ti $2p_{3/2}$ and the O 1s binding energies are compiled along with the XPS-derived atomic ratios Ti/Si and Pd/(Ti + Si). The binding energy of the Si 2p is 104.3 ± 0.1 eV for all the samples and is typical of the value of pure silica [21]. With the exception of Pd/TiO_2, characterized by a Pd $3d_{5/2}$ binding energy of 336.9 eV, the binding energy of Pd $3d_{5/2}$ in all the other fresh catalysts is 337.4 ± 0.1 eV. This value coincides with Pd^{4+} in PdO_2 [22–23]. This oxide has been reported to be present on different supports [10,23]. Its formation may be attained by oxygen incorporation into the PdO crystal lattice during calcination [23]. The Ti 2p spectra of the different samples shown in Fig. 7 are characterized by the two spin–orbit components, Ti $2p_{3/2}$ and Ti $2p_{1/2}$, 5.7 eV apart. The binding energy of the Ti $2p_{3/2}$ in the pure TiO_2-supported Pd catalyst is 458.9 eV which is in accordance with a Ti^{4+} species [24]. An increase of this energy is observed in the mixed oxide samples, to a large extent in those with low Ti loading where shifts up to 1.6 eV are found. Two contributions may be responsible for such a significant chemical shift, a "final state" and an "initial state effect". As to the former effect, it accounts for most of the Ti $2p_{3/2}$ chemical

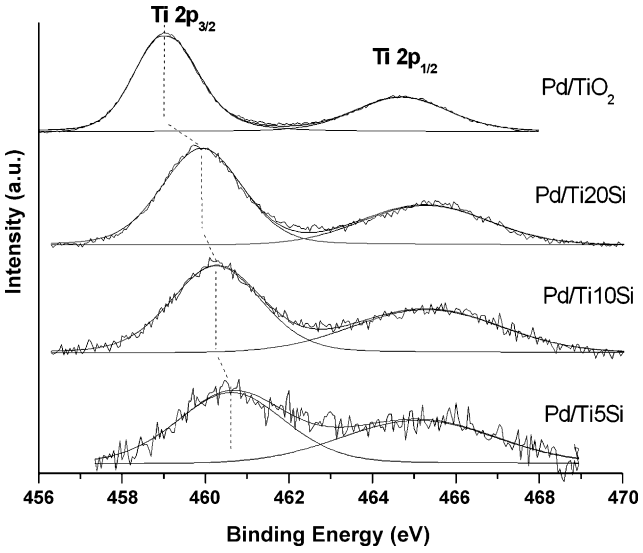

Fig. 7. Ti 2p XP spectra of titania-containing Pd/SiO_2 catalysts.

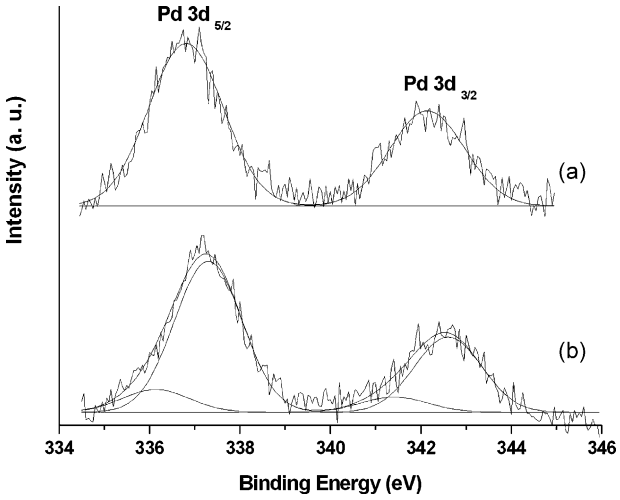

Fig. 8. Pd 3d XP spectra of Pd/TiO_2, (a) fresh sample and (b) after overnight treatment in 10 vol. ppm SO_2/He at 350 °C.

shift when moving from Pd/Ti*x*Si to Pd/TiO_2 [25]. It consists in the extra atomic relaxation energy [26] which is related to the polarizability of the carrier. The less mobile the electrons are, as in SiO_2, the smaller is the relaxation energy and therefore the larger is the measured binding energy of the photoelectrons. The second effect mainly accounts for the larger binding energy observed in samples of low Ti loading as compared to those of high loading [27]. As already observed for a series of TiO_2-grafted SiO_2 [19,21–24], a shift up to 0.7 eV reflects an intimate association of TiO_2 and silica producing Ti–O–Si bonds where Ti^{4+}, with a small increase of the positive charge as compared to Ti–O–Ti, occupies tetrahedral coordination sites similar to Si in SiO_2 [19]. With increasing amounts of TiO_2 the Ti $2p_{3/2}$ binding energy decreases, probably because of the increasingly larger contribution of Ti–O–Ti bonds when moving to pure TiO_2. As observed in Fig. 7, the increasing Ti $2p_{3/2}$ line width of the mixed oxide-supported catalysts as compared to that of Pd/TiO_2 can be attributed to the different titanium local environment present in the mixed samples. The O 1s binding energies at 533.3 ± 0.2 eV and 530.3 eV are typical of SiO_2 and TiO_2, respectively. The second component present in the mixed oxides at 531.2 ± 0.1 eV can be reasonably assigned to oxygen in Si–O–Ti bonds at the surface [21].

The Ti/Si atomic ratios given in Table 4 increase with rising amounts of TiO_2. Yet they always remain lower than the corresponding bulk values given in parentheses. Such discrepancies in TiO_2/SiO_2 are frequently observed, and quite independent of the preparation methods employed (mixed oxides or supported oxides) [27]. Some inadequacy in the sensitivity factors may account for such differences, however, since the catalysts with the highest titania content exhibit the largest discrepancies, spatial inhomogeneities during the sol–gel catalyst synthesis, e.g. TiO_2 agglomeration, cannot be excluded to play a role as well. Moreover, the Pd/(Ti + Si) atomic ratios listed in Table 4 are all quite different although a constant value for all samples would have been expected on the basis of the XRF analyses. Different support texture (in terms of surface area and pore size) may account for the difference in the XPS intensity peak and therefore for the derived atomic concentration. As given in Table 4, large discrepancies in Pd/(Ti + Si) atomic ratios are also obtained for the aged samples. Moreover, the overall decrease of these values (given in parentheses) may indicate either palladium particle sintering or palladium inward diffusion. According to the XRD patterns suggesting good particle dispersion especially for the highest titania loading, diffusion of the palladium through the support porous structure may have occurred.

To investigate possible SO_2-induced chemical changes, XPS analyses of the samples were carried out after the overnight treatment in SO_2 at 350 °C. Similarly to PdO supported on siliceous HMS [10], no significant Pd 3d binding energy shift associated with the possible formation of $PdSO_4$ was detected in both the pure oxide and the mixed oxide catalysts. Only in the case of Pd/TiO_2, see Fig. 8, a positive shift of about 0.4 eV and an additional small Pd component at the lower binding energy of Pd $3d_{5/2}$ at 336.0 eV were observed. The higher energy component at 337.3 eV was still lower than the Pd $3d_{5/2}$ binding energy of the reference $PdSO_4$ for which a value of ~339 eV in accord with literature [7] was obtained. The value at 336.0 eV was typical of a more reduced form of Pd. It is worth noting that similar Pd spectrum was obtained also after SO_2 treatment in the presence of oxygen. For all the treated samples, a broad S 2p peak at ~170.0 eV, characteristic of SO_4^- was present. However, whereas in the case of Pd/SiO_2 and Pd/Ti*x*Si the intensity of this peak decreased strongly with time [10], a rather stable signal was obtained for Pd/TiO_2. On the other hand, the Ti $2p_{3/2}$ binding energy of none of the samples was not observed to vary due to the SO_2 treatment. Considering that the Pd 3d spectra ruled out the formation of $PdSO_4$, and that the Ti 2p binding energy for the sulfated and unsulfated TiO_2 are expected to be the same [28], it seems quite plausible, on the bases of these XPS data, to associate the presence of sulfate with the titania support.

To further confirm some of the above conclusions, in particular the presence of the Si–O–Ti linkages and the sulfation of Ti(IV), FT-IR measurements were performed. In Fig. 9 the spectra of the pure and mixed Ti*x*Si oxides are shown. The SiO_2 spectrum is characterized mainly by a strong band at 1110 cm^{-1} and smaller peaks at 807 and 470 cm^{-1} which can be attributed, in order of mention, to the asymmetric stretching, symmetric stretching and bending of bulk Si–O–Si [29]. The weak band at 970 cm^{-1} is due to the Si–OH stretching vibration of surface silanol groups [29]. On the other hand, the spectrum of pure TiO_2 is characterized by a broad band centered at ~600 cm^{-1} which is attributed to bulk Ti–O–Ti. The peak at 951 cm^{-1}, observed only in the mixed oxides, can thus be attributed to the Si–O–Ti vibration mode [29–30]. In this way, we confirm the formation of the mixed oxide linkage. The FT-IR spectra of the catalysts after overnight treatment with SO_2 at 350 °C were also measured. Only the spectrum of Pd/TiO_2, given in Fig. 10, contained some bands attributable to SO_4^-, thus confirming the above XPS suggestion. Indeed, in the range between 1400 and 1000 cm^{-1}, four main bands are present. As reported in

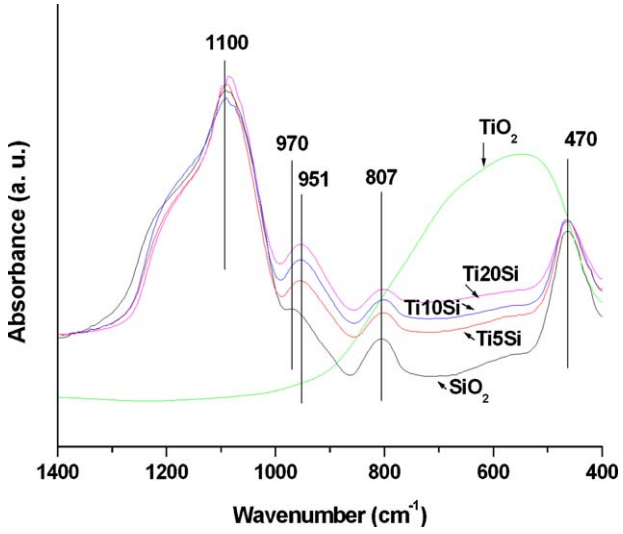

Fig. 9. Infrared spectra for pure oxides and mixed Ti*x*Si supports.

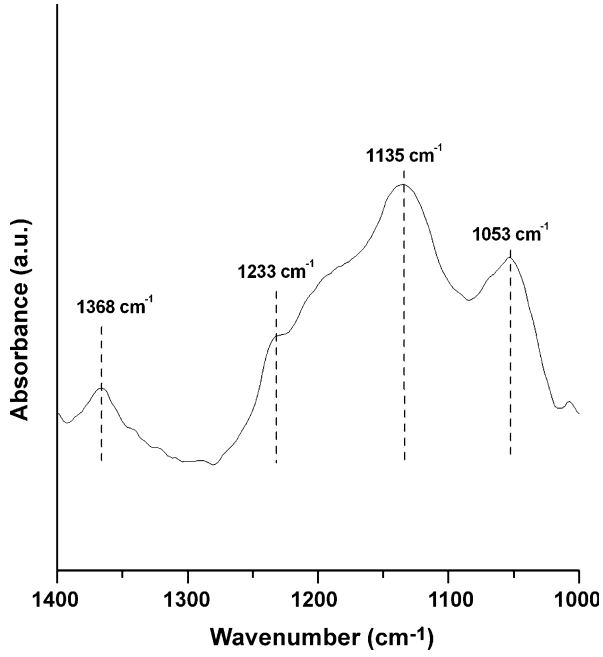

Fig. 10. Infrared spectra of Pd/TiO_2 after overnight treatment in 10 vol.% SO_2/He at 350 °C.

the literature, the band at 1368 cm^{-1} can be attributed to the stretching frequency of S=O [28]. The other peaks are characteristic of SO_4^{-} bound to TiO_2 with a configuration of either chelating bidentate or bridged bidentate [28].

4. Summary

Various Pd-based catalysts were tested in methane oxidation in absence and in the presence of SO_2. The performance of these catalysts was compared on the basis of the temperature-dependent conversion and a respective analysis of the T_{50} values. In the absence of SO_2, "PdO" on mixed oxide supports, SiO_2–TiO_2, with amounts of Ti/Si varying between 5 and 20 wt%, show higher activity than those on pure oxide supports. In comparing PdO on pure oxide supports, TiO_2 and SiO_2, it turns out that TiO_2 yields lower T_{50} values than SiO_2. This is in accordance with a lower apparent activation energy indicative of a superior intrinsic activity and also in accord with a better PdO dispersion as detected by XRD. The two catalysts yet behave quite differently under SO_2 poisoning conditions. As shown by XPS and FT-IR, Pd/TiO_2 is easily sulfated but maintains a higher activity than Pd/SiO_2. The inertness of silica favors the poisoning of the active phase due to the preferential interaction of SO_2 with PdO [10]. The presence of SO_2 during methane oxidation actually has a twofold effect. It can reduce PdO to provide less active Pd metal and it chemisorbs on active sites of the PdO phase thus forming sites that are less efficient in C–H activation [3]. Under severe poisoning conditions through overnight exposure of the catalysts to SO_2 at 350 °C, Pd/SiO_2 deactivates but not as much as Pd/TiO_2 and, different from the latter, it may be regenerated in subsequent catalytic runs of methane oxidation. Such opposite behavior can be explained by the stronger interaction of SO_2 with TiO_2, forming titanium sulfates, followed by the saturation of the support adsorption sites during the overnight treatment and consequent spillover of the SO_x species to the PdO during the following SO_2-free methane oxidation run. This scenario is absent in Pd/SiO_2 for which the final temperature (600 °C) adopted in all catalytic runs is high enough to quickly remove the SO_2 so as to recover the active sites.

The addition of up to 20% TiO_2 to the SiO_2 support via the sol–gel method causes a promotional effect in the catalytic performance of the PdO particles. An optimal performance was seen for 10 wt% TiO_2. More precisely, a promotional effect was found consisting of an increase of the methane oxidation activity (lower T_{50}), an increasing resistance towards SO_2 poisoning and a substantial activity improvement of the catalyst in successive catalytic runs. The first of these effects is associated with an increased Pd intrinsic activity. As proven by XPS and FT-IR, the mixed oxide supports are characterized by the presence of Si–O–Ti linkages which, according to literature, correspond to redox sites with the highest specific catalytic activity for oxidation reactions [21,27,31]. The replacement of a Ti ion by a Si ion in such a linkage was previously suggested to determine an increased Ti(IV) oxidation potential that in the present case enhances the oxygen mobility at the interface between the Ti–O–Si unit and the PdO particles. Such oxygen mobility would favor, during the reaction, the formation of site pairs consisting of adjacent surface Pd–PdO species where methane dissociation could occur [32]. Such an effect is most pronounced at relatively low TiO_2 loading since, according to the structural data, the contribution of the above-mentioned interface would be stronger as compared to samples with too high TiO_2 content where islands of TiO_2 would form. The second promotional effect consists in a superior tolerance with respect to SO_2 either added during the reaction or He-diluted in a pretreatment at 350 °C. The combination of the sulfatable TiO_2 acting as SO_2 scavenger during reaction, and the unsulfatable and high surface area SiO_2, allowing for the easier removal of sulfur-containing species after prolonged exposure to SO_2 with or without oxygen, seems to provide the reason for the TiO_2 promotion effect. Moreover, the noticeable increase in activity of the TiO_2-promoted catalysts with respect to the fresh samples, after the long-term treatment in SO_2 is possibly due to a dynamic equilibrium between reduced and oxidized states of palladium.

5. Conclusion

The modification of silica by small amounts of titania (5–10 wt%) has a substantial effect on the methane oxidation performance and on the SO_2 tolerance of supported PdO. The increased methane conversion with respect to the pure oxide supported catalysts can be associated with the formation of Si–O–Ti linkages increasing the intrinsic activity of the supported PdO.

The combination of the right quantities of two chemically different oxides like TiO_2 and SiO_2 increases the tolerance of the PdO phase towards poisoning by SO_2. The remarkable reactivation/promotion upon SO_2 treatment can be likely attributed to the SO_2-induced reduction and structural rearrangement of the PdO phase. The high CH_4 conversion activity obtained over the Pd/Ti10Si after five consecutive runs and after heavy exposure to SO_2 may have practical implications in future catalyst design.

Acknowledgements

Support by European Community, Network of Excellence (NoE) IDECAT (Integrated Design of Catalytic Nanomaterials for Sustainable Production) and COST D36 action is acknowledged. G. Melaet is grateful for a FRIA grant of the FNRS (Fonds National de la Recherche Scientifique) de la communité francaise de Belgique.

References

[1] P. Gelin, M. Primet, Appl. Catal. B 39 (2002) 1.
[2] F. Arosio, S. Colussi, G. Groppi, A. Trovarelli, Catal. Today 117 (2006) 569.
[3] K. Fujimoto, F.H. Ribeiro, M.A. Borja, E. Iglesia, J. Catal. 179 (1998) 431.
[4] H. Yoshida, T. Nakajima, Y. Yazawa, T. Hattori, Appl. Catal. B 71 (2007) 70.
[5] M. Shmal, M.M.V.M. Souza, V.V. Alegre, M.A. Pereira da Silva, D.V. Cesar, C.A.C. Perez, Catal. Today 118 (2006) 392.
[6] L.M.T. Simplicio, S.T. Brandao, E.A. Sales, L. Lietti, F. Bozon-Verduraz, Appl. Catal. B 63 (2006) 9.
[7] D.L. Mowery, R.L. Mc Cormick, Appl. Catal. B 34 (2001) 287.
[8] L.J. Hoyos, H. Praliad, M. Primet, Appl. Catal. A 98 (1993) 125.
[9] L.F. Liotta, G. Di Carlo, G. Pantaleo, A.M. Venezia, G. Deganello, Appl. Catal. B 66 (2006) 217.
[10] A.M. Venezia, R. Murania, G. Pantaleo, G. Deganello, J. Catal. 251 (2007) 94.
[11] P. Gelin, L. Urfels, M. Primet, E. Tena, Catal. Today 83 (2003) 45.
[12] G. Pecchi, P. Reyes, I. Concha, J.L.G. Fierro, J. Catal. 179 (1998) 309.
[13] JCPDS Powder Diffraction File Int. Centre for Diffraction Data, Swarthmore.
[14] H.P. Klug, X-ray Diffraction Procedure for Polycrystalline and Amorphous Materials, Wiley, New York, 1954.
[15] S.J. Gregg, K.S. Sing, Adsorption, Surface Area and Porosity, 2nd ed., Academic Press, San Diego, 1982.
[16] V. La Parola, G. Deganello, S. Scirè, A.M. Venezia, Solid State Chem. 174 (2003) 482.
[17] K. Lambert, M.S. Kazi, R.J. Farrauto, Appl. Catal. B 14 (1997) 211.
[18] R. Burch, F.J. Urbano, P.K. Loader, Appl. Catal. A 123 (1995) 173.
[19] R. Castillo, B. Koch, P. Ruiz, B. Delmon, J. Catal. 161 (1996) 524.
[20] S.T. Tauster, S.C. Fung, R.L. Garten, J. Am. Chem. Soc. 100 (1978) 170.
[21] A.M. Venezia, F.L. Liotta, G. Pantaleo, A. Beck, A. Horvath, O. Geszti, A. Kocsonya, L. Guczi, Appl. Catal. A 310 (2006) 114.
[22] D.H. Kim, S.I. Woo, J.M. Lee, O.B. Yang, Catal. Lett. 70 (2000) 35.
[23] Y. Bi, G. Lu, Appl. Catal. B 41 (2003) 279.
[24] E. Santacesaria, M. Cozzolino, M. Di Serio, A.M. Venezia, R. Tesser, Appl. Catal. A 270 (2004) 177.
[25] G. Lassaletta, A. Fernandez, J.P. Espinòs, A.R. Gonzalez-Elipe, J. Phys. Chem. 99 (1995) 1484.
[26] C.D. Wagner, Faraday Discuss. Chem. Soc. 60 (1975) 291.
[27] X. Gao, I.E. Wachs, Catal. Today 51 (1999) 233.
[28] J.P. Chen, R.T. Yang, J. Catal. 139 (1993) 277.
[29] Y.M.M. Mohamed, T.M. Salama, T. Yamaguchi, Colloid Surf. A 207 (2002) 25.
[30] Y. Kong, X. Guo, F. Zhang, S. Jiang, J. Wang, Y. Lu, Q. Yan, Mater. Lett. 59 (2005) 3099.
[31] S. Srinivasan, A.K. Datye, M. Hampden-Smith, I.E. Wachs, G. Deo, J.M. Jehng, A.M. Turek, C.H.F. Peden, J. Catal. 131 (1991) 260.
[32] R. Burch, D.J. Crittle, M.J. Hayes, Catal. Today 47 (1999) 229.